Modeling antigen-specific T cell dynamics following Hepatitis B Vaccination indicates differences between conventional and regulatory T cell dynamics

Peer-reviewed author version

Besbassi, Hajar; Elias, George; Meysman, Pieter; Jansens, Hilde; Laukens, Kris; Van Damme, Pierre; HENS, Niel; Beutels, Philippe & OGUNJIMI, Benson (2024) Modeling antigen-specific T cell dynamics following Hepatitis B Vaccination indicates differences between conventional and regulatory T cell dynamics. In: Vaccine, 42 (21) (Art N° 126148).

DOI: 10.1016/j.vaccine.2024.07.049
Handle: http://hdl.handle.net/1942/44271

Modeling Antigen-Specific T Cell Dynamics Following Hepatitis B Vaccination indicates differences between conventional and regulatory T cell dynamics

Hajar Besbassi[1,2,3,*], George Elias[2,4], Pieter Meysman[2,5], Hilde Jansens[6], Kris Laukens[2,5], Pierre Van Damme[2,7], Niel Hens[1,8], Philippe Beutels[1,†], and Benson Ogunjimi[1,2,3,9,†]

[1]Centre for Health Economics Research & Modeling Infectious Diseases (CHERMID), Vaccine & Infectious Disease Institute (VAXINFECTIO), University of Antwerp, Antwerp, Belgium
[2]Antwerp Unit for Data Analysis and Computation in Immunology and Sequencing (AUDACIS), University of Antwerp, Antwerp, Belgium
[3]Antwerp Center for Translational Immunology and Virology (ACTIV), Vaccine & Infectious Disease Institute (VAXINFECTIO), University of Antwerp, Antwerp, Belgium
[4]Laboratory of Experimental Hematology (LEH), Vaccine and Infectious Disease Institute, University of Antwerp, Antwerp, Belgium
[5]Adrem Data Lab, Department of Mathematics and Computer Science, University of Antwerp, Antwerp, Belgium
[6]Department of Clinical Microbiology, Antwerp University Hospital, Antwerp, Belgium
[7]Centre for the Evaluation of Vaccination (CEV), Vaccine & Infectious Disease Institute (VAXINFECTIO), University of Antwerp, Antwerp, Belgium
[8]Data Science Institute (DSI), Interuniversity Institute for Biostatistics and statistical Bioinformatics (I-BioStat), UHasselt, Hasselt, Belgium
[9]Department of Paediatrics, Antwerp University Hospital, Edegem, Belgium
[*]Corresponding author. Email: hajar.besbassi@uantwerpen.be
[†]These authors contributed equally to this work

Abstract:

Our study aims to investigate the dynamics of conventional memory T cells (Tconv) and regulatory T cells (Treg) following activation, and to explore potential differences between these two cell types. To achieve this, we developed advanced statistical mixed models based on mathematical models of ordinary differential equations (ODE), which allowed us to transform post-vaccination immunological processes into mathematical formulas. These models were applied to in-house data from a de novo Hepatitis B vaccination trial. By accounting for inter- and intra-individual variability, our models provided good fits for both antigen-specific Tconv and Treg cells, overcoming the challenge of studying these complex processes. Our modeling approach provided a deeper understanding of the immunological processes underlying T cell development after vaccination. Specifically, our analysis revealed several important findings regarding the dynamics of Tconv and Treg cells, as well as their relationship to seropositivity for Herpes Simplex Virus Type 1 (HSV-1) and Epstein-Barr Virus (EBV), and the dynamics of antibody response to vaccination. Firstly, our modeling indicated that Tconv dynamics suggest the existence of two T cell types, in contrast to Treg dynamics where only one T cell type is predicted. Secondly, we found that individuals who converted to a positive antibody response to the vaccine earlier had lower decay rates for both Tregs and Tconv cells, which may have important implications for the development of more effective vaccination strategies. Additionally, our modeling showed that HSV-1 seropositivity negatively influenced Tconv cell expansion after the second vaccination, while EBV seropositivity was associated with higher Treg expansion rates after vaccination. Overall, this study provides a critical foundation for understanding the dynamic processes underlying T cell development after vaccination.

Keywords: Immune system, T cell dynamics, Mathematical models, Mixed-effects modeling, Vaccination , Statistics.

1 Introduction

The immune system plays a crucial role in protecting the body against pathogens and preventing the development of diseases. It is a complex system consisting of various types of cells and molecules that work together to identify and eliminate foreign invaders while maintaining self-tolerance. Among the key players of the immune system are T cells, which play a central role in orchestrating immune responses against pathogens and cancer cells[1,2]. Memory T cells, both conventional and regulatory, are subtypes of T cells that provide long-lasting protection against previously encountered antigens and modulate immune responses, respectively[3,4]. While the HBV vaccine primarily elicits an antibody response, the role of memory T cells is pivotal in sustaining long-term immunity. These cells aid in the rapid recall response to HBV upon re-exposure and are crucial in maintaining a balanced immune state. This study emphasizes the understudied yet significant role of memory T cells in the context of HBV vaccination, bridging a gap in current vaccine immunology research. Conventional memory T cells are responsible for the rapid and robust response to pathogens upon re-exposure, while regulatory T cells suppress immune responses and prevent excessive inflammation and tissue damage[3,4]. The development and maintenance of memory T cells are complex processes that involve various factors such as cytokines, co-stimulatory molecules, and transcription factors[5,6].

Vaccination is a highly effective strategy for generating memory T cells and protecting individuals from infectious diseases[7]. For example, the hepatitis B virus (HBV) vaccine induces the production of memory T cells and antibodies against the virus, providing long-term protection against HBV infection[8]. Using data from a previously published study[9], we build upon existing mathematical frameworks to develop mixed-effects models that capture the dynamics of Tconv and Treg following hepatitis B vaccination. Anti-hepatitis B surface antibodies (Anti-HBs) are proteins produced by the immune system in response to the presence of the hepatitis B surface antigen (HBsAg). Anti-HBs concentrations more than 10 mIU/mL provide protection against infection. However, it is worth noting that the percentage of individuals maintaining anti-HBs levels above 10 mIU/mL is significantly influenced by the duration since the initial vaccination. Anti-HBs concentrations below this threshold may not confer the same level of protection against HBV infection. It is important to recognize that the 10 mIU/mL threshold is a commonly used indicator of protection, although it is not an absolute cutoff. Our models aim to reflect the individual variability observed in the development of these memory responses and to provide a mechanistic understanding that can inform vaccination strategies. Memory specific T cells prompt a powerful anamnestic response upon exposure to the hepatitis B virus, preventing acute illness, long-term viremia, and chronic infection. An anamnestic anti-HBs response following vaccination with an additional dose demonstrates specific memory T cells after hepatitis B vaccination[10]. The majority of individuals who had a favorable response to the initial series of vaccinations will experience a rapid rise in anti-HBs as a result of this booster dose. Time since first vaccination appears to be related to immune memory persistence[11]. Although progress has been made in the development of vaccines against hepatitis B virus (HBV), the long-term clinical outcome of the disease remains poor due to the challenge of achieving immunological memory, which may involve viral clearance and/or non-specific antibody response[9,12].

Recently, several mathematical models were developed to model longitudinal immune responses using ordinary differential equations (ODEs), which are popular and powerful tools for modelling very complex dynamical systems in many fields. They are widely used in the study of population dynamics, epidemiology, virology, pharmacokinetics and gene regulatory networks because of their ability to describe key interaction mechanisms between biological components of complex systems, their evolution over time, and provide reasonable stochastic dynamics approximations[13–17]. Our study extends these methods by applying mixed-effects modeling to account for both within- and between-subject variability in T cell

responses. Mixed-effects modeling offers the benefit of accounting for and quantifying the correlation between several replicates, as well as of achieving a more precise parameter estimate by pooling all the data, in comparison to fixed-effects modelling. There is currently a growing interest in estimating mixed-effects ODE models due to their ability to account for both within- and between-subject variability. With repeated measurements from multiple individuals, mixed-effects ODE models provide a more robust way of estimating model parameters than traditional ODE models. As a result, there is a growing interest in developing and applying mixed-effects ODE models in immunology research. The first to use the mixed effects modeling method with ordinary differential equations (ODE) in a form that more closely approximated immune response dynamics after vaccination were Andraud et al.[16], who focused on long-term impacts, and Le et al.[18] on the immediate effects of vaccination. Furthermore, Keersmaekers et al.[19] used the mixed effect modeling to investigate two vaccine doses. Another recent study by Besbassi et al.[20] employed mixed-effects ODE models to examine antibody dynamics following re-exposure to infection. The approach was applied to 61 herpes zoster patients to gain insights into varicella-zoster virus specific antibody dynamics during and after clinical herpes zoster. The study provided a deeper understanding of the population's characteristics and offered unique insights that can aid in improving our understanding of Varicella-Zoster Virus (VZV) antibody dynamics and in making more accurate projections regarding the potential impact of vaccines[21].Our work complements these studies by focusing on the dynamics of memory T cell populations, a less explored aspect of the immune response to vaccination.

In this current study, we have applied an innovative ODE-based mixed-effects modeling approach to analyze the kinetics of hepatitis B virus (HBV)-specific memory T cell responses in individuals receiving de novo HBV vaccination[9]. Our focus on characterizing the dynamics of both conventional and regulatory memory T cells over time aims to unravel the complexities underlying immunological memory development and maintenance. By considering individual variability in these responses, our work sheds light on key factors that drive the long-term efficacy of vaccines and could significantly influence the design of future vaccination strategies and the development of novel immunotherapies.

This research aligns with the evolving landscape of immunological modeling, extending beyond traditional methodologies to offer a more nuanced understanding of T cell dynamics post-vaccination. Our integration of advanced mixed-effects modeling with a specific focus on memory T cells offers a novel perspective critical for comprehending vaccine-induced immune responses. The insights gained from this study are not only pivotal for advancing vaccine development but also provide a valuable framework for further explorations in the field of vaccine immunology. Specifically, this study aims to model the dynamics of memory T cells post-Hepatitis B vaccination, with a focus on the roles of conventional memory T cells (Tconv) and regulatory memory T cells (Tregs), exploring their responses to vaccination and how they contribute to long-term immunity.

The approach of this study is novel, leveraging the power of mixed-effects modeling to delve into the intricacies of immune response variability among individuals. This methodology allows for a more accurate depiction of the complex interplay between various immunological factors and the hepatitis B vaccine, setting a new standard for the quantitative analysis of vaccine efficacy and immune memory dynamics.

2 Material and methods

2.1 Data

We used data from a previously published study by Elias et al.[9], which included a cohort of 34 healthy subjects who received the hepatitis B vaccine. The absence of prior HBV infection and vaccination history in this cohort provides an ideal baseline for our analysis, allowing for a clearer understanding of T cell

dynamics in response to the hepatitis B vaccine. This data selection from Elias et al.[9] study is pivotal for our analysis, as it provides a rich source of empirical evidence necessary for understanding the nuanced T-cell responses post-vaccination, particularly focusing on TCR affinity and seropositivity, which are key determinants of vaccine efficacy. Engerix-B® with a dose of 20 μg of hepatitis B surface antigen with alum adjuvant, was administered to the participants through intramuscular injection on days 0, 30, and 365. Peripheral blood samples were collected at four time points: day 0 (pre-vaccination), as well as 3 months, 6 months, and 12 months after the first vaccine dose. The blood samples at the 12-month mark were collected just before the administration of the third dose on day 365. This timing ensures that the measurements reflect the immune response from the first two doses without the influence of the third dose. The cohort exhibited a diverse age range, from 21.3 to 50.2 years, and comprised 22 females and 12 males. Participants were categorized as early-converters if they seroconverted by day 60, late-converters if seroconversion occurred by day 180 or day 365, and non-converters if their anti-HBs titer did not exceed 10 IU/ml at any measured time points. This comprehensive data collection enables a thorough investigation of the dynamic immune response to the hepatitis B vaccine over a one-year period.

The study also collected data on the TCR affinity for the HBsAg peptide pool and cytomegalovirus (CMV), ebstein-barr virus (EBV), or herpes simplex virus type 1 (HSV) seropositivity during the study. The TCR affinity, specifically the HBsAg-specific TCR affinity, was determined by calculating the ratio of unique T-cell receptors (TCRs) annotated as HBsAg-specific in the sequenced TCR repertoire to the number of bystander TCRs. This calculation provides insight into the strength of the binding interaction between the T-cell receptor and the peptides derived from the hepatitis B surface antigen. CMV, EBV, and HSV seropositivity were measured at the day of vaccination to evaluate whether previous exposure to these viruses influenced the immune response to the hepatitis B vaccine. These factors were included to comprehensively assess how prior viral exposures might affect vaccine efficacy. The data collected was used to study the longitudinal dynamics of $CD4^+$ T cells and to evaluate the influence of these factors on the immune response to the hepatitis B vaccine.

2.2 T-cell data

Generating adaptive immune responses against microbial invaders is mostly dependent on $CD4^+$ T cells. The identification of antigenic peptides presented on major histocompatibility complexes (MHC) by the TCR, together with antigen-independent co-stimulation, is necessary for naive $CD4^+$ T cells to develop into more specialized subsets after T cell activation. The study utilized flow cytometry to assess T cell responses and TCRβ repertoire sequencing to identify vaccine-specific TCRβ clonotypes. In our focus, we particularly concentrated on two subsets of $CD4^+$ T cells stimulated by HbsAg: memory conventional T cells (Tconv) and regulatory memory T cells (Tregs), defined by distinct surface markers. Depending on the antigen, $CD4^+$ T cells can differentiate into a variety of subset populations. In the previously published study[9] HbsAg stimulated $CD4^+$ T cells were subtyped into different cell subsets; however, we will only focus on two types: one being the memory conventional T cell subset out of total $CD4^+$ T cell ("Tconv"), which is defined as $CD154^+CD137^-$ cells. The other being regulatory memory T cells out of total $CD4^+$ T cells ("Tregs"), which is defined as $CD154^-CD137^+$ cells, that specialise in immunological homeostasis and maintenance of self-tolerance, inflammation control and prevention of autoimmune diseases. These subsets were chosen due to their significant roles in the immune response to hepatitis B vaccination. The use of CD154 and CD137 as markers for identifying these subsets has been validated in previous studies, demonstrating their efficacy in characterizing T cell responses[9,22].

To accurately capture the dynamics of these T-cell populations, we introduce two pivotal time points, h_1 and h_2, which delineate the phases of T-cell population changes post-vaccination. The period $[0, h_1]$ encompasses the initial response to the vaccine, characterized by an increase in T-cell counts following

the first dose, with h_1 marking the end of this phase, observed just before the 2-month mark. The second period $[2, h_2]$ extends from the point marking the beginning of the secondary response phase, following the second vaccination dose, up to h_2, the time point at which we observe a plateau or decrease in T-cell populations, indicating the stabilization of the immune response. This secondary phase captures the sustained or boosted immune response, culminating at 12 months post-initial vaccination. In case only one peak is observed in the T-cell response dynamics, we will assume $h_1 = 2 < h_2$, which allows for a flexible adaptation of our analysis framework to the observed data patterns. These defined periods are instrumental in our study as they allow us to segment the immune response into distinct, quantifiable phases of T-cell dynamics, providing a structured framework for our analysis.

To provide a comprehensive understanding of the participant demographics and key characteristics in our study, Table1 summarizes the essential data. This includes age distribution, antibody titres, TCR affinity, serostatus for various viruses, gender distribution, and vaccine response status. This diverse representation of participants ensures a comprehensive analysis of the immune response to the hepatitis B vaccine. Figures 1 and 2 show individual-specific memory Tconv and Treg profiles by time in days, respectively. The data are presented for early, late, and non-converters. These visual representations provide a clear depiction of the dynamic changes in T cell populations across different converter categories and time points, emphasizing the need for individual-level modeling approaches.

Characteristic	**Description**
Age Range	21.3 - 50.2 years (Median: 40.25 years)
Antibody Titre	Range: 2 - 8.55 (Mostly concentrated around 2)
TCR Affinity	Range: 0.42 - 1.46
CMV Status	Positive: 9, Negative: 25
EBV Status	Positive: 25, Negative: 9
HSV1_2 Status	Positive: 14, Negative: 20
HHV6 Status	Positive: 32, Negative: 2
Gender	Female: 22, Male: 12
Vaccine Response	Early-converter: 21, Late-converter: 9, Non-converter: 4

Table 1. Summary of Participant Demographics and Vaccine Response

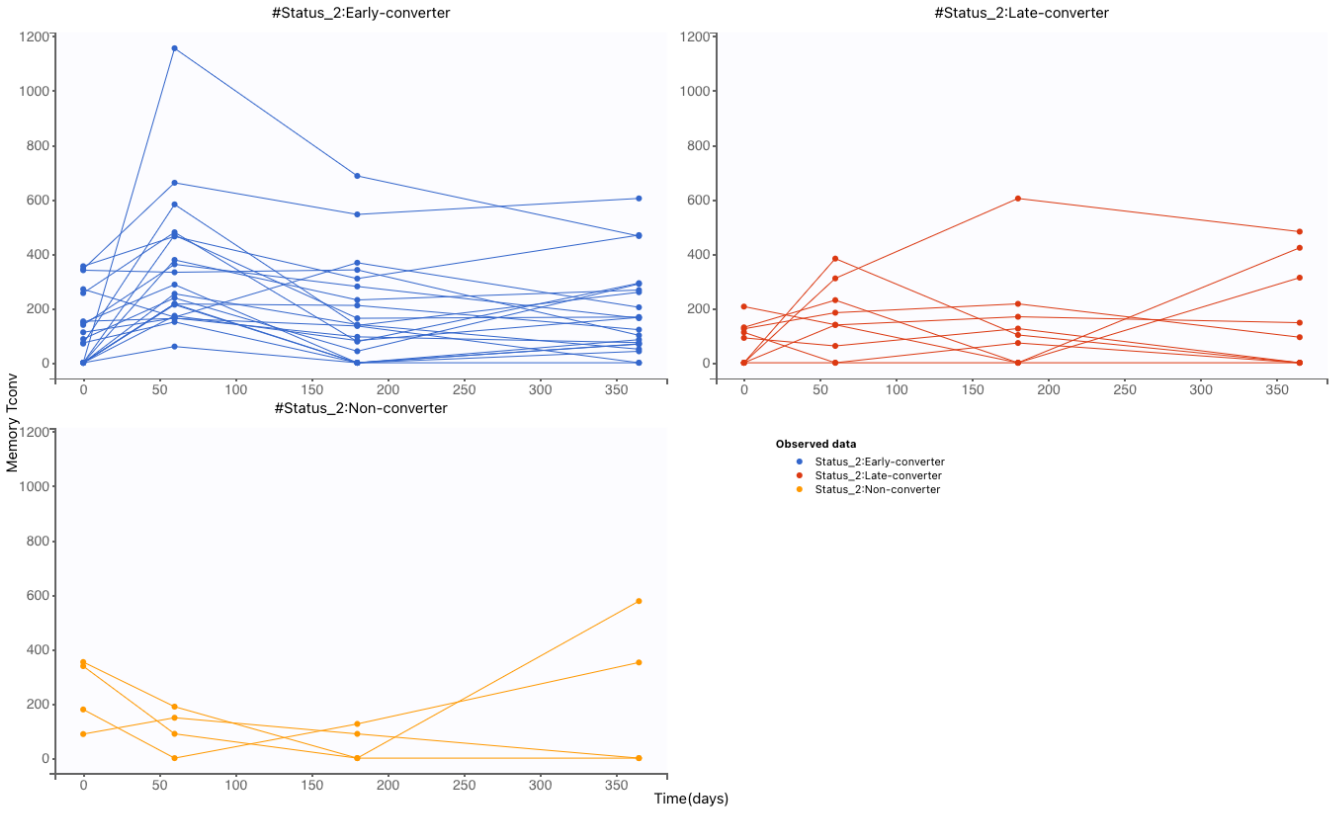

Figure 1. Individual-specific memory Tconv profiles by time (in days) for Early/Late/Non converter status. The plot shows the variation in memory Tconv over time for each individual, and how this varies between early converters, late converters, and non-converters.

2.3 Mathematical methods

2.3.1 T-cell dynamic Models

In this subsection, we present nonlinear mixed-effect models based on ordinary differential equations to model the dynamics of T-cells. Our goal is to obtain models that best describe the available data while representing the important cell populations in the T-cell response process generated by the body after vaccination. This includes accounting for the distinct roles and lifespans of short-lived and long-lived T-cell populations, which are derived from empirical observations and theoretical insights into T-cell dynamics post-vaccination.

Our modeling strategy has been developed with an awareness of the current state of T cell dynamics research. We have carefully reviewed and considered recent advances in the field, ensuring our models reflect the known biological processes of T cell activation and memory formation post-vaccination. This approach allows us to capture the essential dynamics of T cell responses in a manner that balances biological accuracy with computational and data practicality.

The main T-cell populations considered include conventional memory T cells, regulatory memory T cells, which are key components in understanding the immune response. These are further subdivided into short-lived and long-lived memory T conventional cells, and short-lived and long-lived memory T regulatory cells. The differentiation into short-lived and long-lived subsets is based on established immunological knowledge and is crucial for modeling the immediate and memory responses accurately.

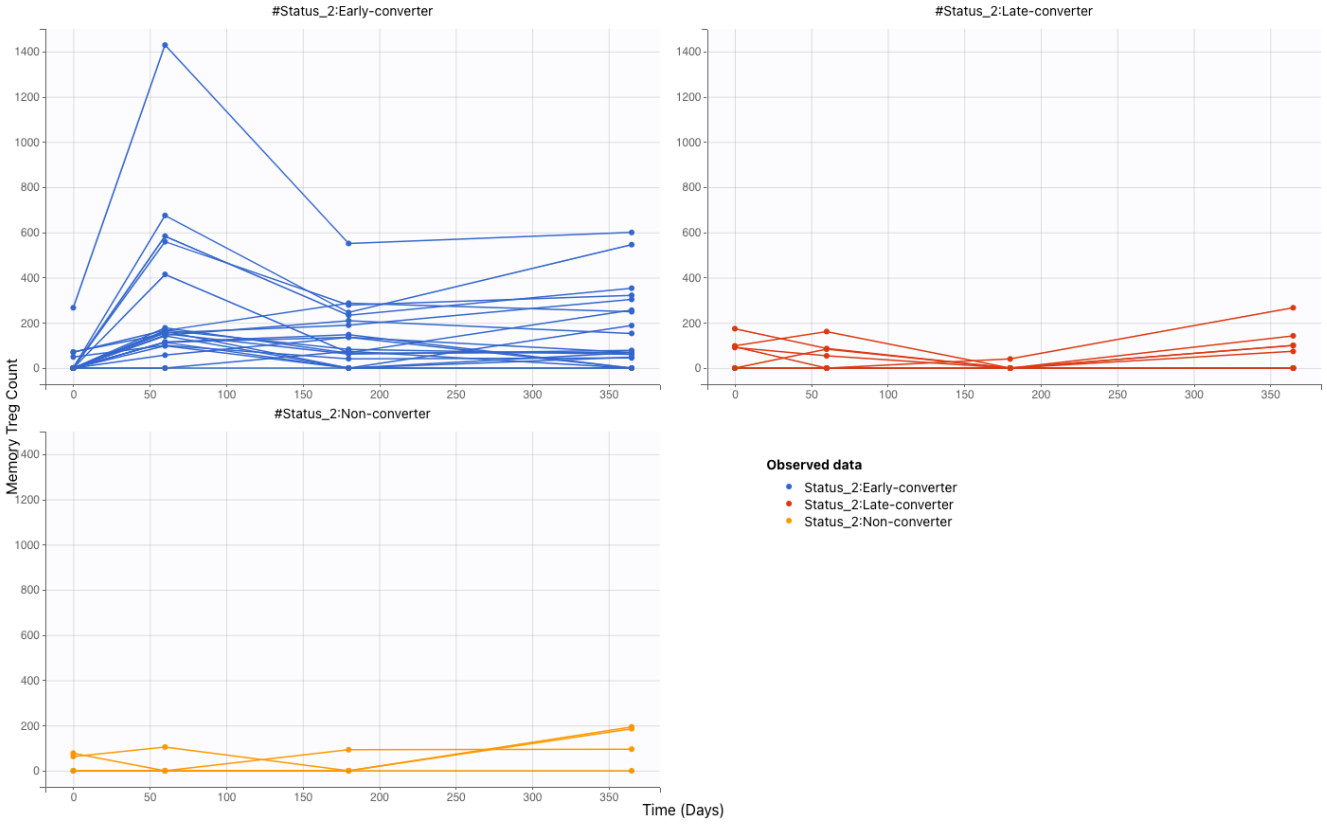

Figure 2. Longitudinal profiles of memory regulatory T-cells over time (in days) for individual participants, stratified by their converter status (Early/Late/Non). The variation in response over time and between individuals is apparent, highlighting the importance of individual-level modeling approaches.

While our models do not explicitly label a process as 'clonal expansion', the mechanism is inherently captured in the dynamic representation of T-cell proliferation and response post-vaccination. The expansion terms in our models implicitly encompass the biological reality of T-cell multiplication in response to antigenic stimulation, which is a cornerstone of the adaptive immune response.

We used a systematic approach to fit and compare multiple models to obtain the least number of parameters needed to accurately describe the T-cell dynamics, ensuring model parsimony and avoiding overfitting. This approach aligns with the principles of model selection where simplicity and accuracy are balanced to avoid complexity that does not add explanatory power. The general ODE equation used to describe the dynamics of T-cells is:

$$\begin{cases} \dfrac{dT}{dt} & = \varphi_1(T) I_{0\leq t\leq h_1} + \varphi_2(T) I_{2\leq t\leq h_2} - \varphi_3(T), \\ T_0 & = T(0), \qquad t = 0 \end{cases}$$

Here, φ_1 represents the expansion of T-cells after the first vaccination at time 0 until a certain time h_1 (with $0 \leq h_1 \leq 2$). The inclusion of different phases of T-cell expansion reflects the observed immune response kinetics following vaccination. After h_1 has been reached, T-cells will not further be activated until the second vaccination, one month after the first one, which φ_2 defines as the expansion of T-cells during the period $[2, h_2]$, h_2 being the point at which the second T-cell peak is attained.

In the context of our study, $I_{0\leq t\leq h_1}$ denotes the active phase of T-cell proliferation following the initial vaccination, where t is the time post-vaccination and h_1 is the time until which this immediate response is considered. The second term, $I_{2\leq t\leq h_2}$, captures the T-cell expansion from two months post-initial vaccination until the time h_2, which is determined by the observed data to be the point where the T-cell count starts to reduce after the booster-induced peak. These indicators are crucial for our model as they help to segment the T-cell response into distinct phases corresponding to the vaccine administration schedule and observed immunological outcomes.

Our modeling choices are corroborated by empirical data showing distinct phases of T-cell response to vaccination. The decay of T-cells will occur throughout the full time period and is described by the function φ_3. Although not explicitly labeled as 'clonal expansion' in our models, the proliferative behavior of T-cells post-stimulation inherent in these functions encapsulates this biological process. In all models, we assume that the decay rate of T-cells is proportional to the number of T-cells, which can be written as $\varphi_3 = \mu_T \times T$. The proportional decay rate is a common assumption in biological modeling and simplifies the system without loss of generality. Moreover, we assume an expansion rate for T-cells after each vaccination event, which aligns with the initial phase of the immune response characterized by rapid T-cell activation and subsequent division. In this model, one can hypothesize that 1 dividing T-cell will generate 1 circulating "effector" T-cell and 1 T-cell that will proceed in the expansion process.

Assuming an equal expansion rate of T cells after each vaccination leads to Model 1. Functions $\varphi_i (i \in \{1,2,3\})$ can now be written as:

$$\frac{dT}{dt} = \alpha_T I_{0\leq t\leq h_1} + \alpha_T I_{2\leq t\leq h_2} - \mu_T T, \tag{1}$$

This model choice reflects our intention to explore the implications of uniform T-cell proliferation post-vaccination, a scenario that simplifies the biological complexity but offers valuable initial insights. Model 2 does not assume an equal expansion rate after each vaccination. In addition, it is reasonable to consider a different rate after the second vaccination due to a memory response. In this scenario, the functions φ_i are expressed as follows:

$$\frac{dT}{dt} = \alpha_{1_T} I_{0\leq t\leq h_1} + \alpha_{2_T} I_{2\leq t\leq h_2} - \mu_T T, \tag{2}$$

As we proceed, we distinguish the short-lived T cells, denoted as ST(t), from the long-lived T cells, denoted as LT(t). This distinction is not merely for model complexity but is grounded in the biological understanding that different T-cell subtypes exhibit markedly different lifespans and roles in the immune response, as supported by current immunological research[19]. The total T-cell population is represented as the sum of these two distinct sub-populations. While our modeling makes a simplifying assumption about the initial absence of short-lived T cells for tractability, this approach is justified given that our primary interest is in the dynamics post-vaccination. This distinction is vital for accurately capturing the dynamic behavior of T-cell populations during various stages of the immune response, crucial for understanding both immediate and lasting immunity We describe it by the functions φ_i, ψ_i where $i \in \{1,2,3\}$):

$$\begin{cases} \dfrac{dST}{dt} &= \varphi_1(T) I_{0\leq t\leq h_1} + \varphi_2(T) I_{2\leq t\leq h_2} - \varphi_3(T), \\ \dfrac{dLT}{dt} &= \psi_1(T) I_{0\leq t\leq h_1} + \psi_2(T) I_{2\leq t\leq h_2} - \psi_3(T), \\ T(t) &= ST(t) + LT(t), \end{cases}$$

with $LT_0 = LT(0)$ the initial number of long living T-cells and $ST_0 = 0$ the number of short living T-cells at time 0.

First, similarly to the preceding models, we will suppose that the expansion rates of ST are constant and there is no decay of LT (thus a constant number of LT). Model 3 also presumes that the expansion rates of ST after the two vaccinations are identical. The functions φ_i and ψ_i are accordingly given as:

$$\begin{cases} \frac{dST}{dt} & = \alpha_{ST} I_{0\leq t\leq h_1} + \alpha_{ST} I_{2\leq t\leq h_2} - \mu_{ST} ST, \\ \frac{dLT}{dt} & = 0. \end{cases} \tag{3}$$

In Model 4, we consider different expansion rates of ST after the two vaccinations. The decision to explore different expansion rates stems from our hypothesis that post-vaccination immune responses may vary significantly between initial and subsequent exposures. This leads to:

$$\begin{cases} \frac{dST}{dt} & = \alpha_{1_{ST}} I_{0\leq t\leq h_1} + \alpha_{2_{ST}} I_{2\leq t\leq h_2} - \mu_{ST} ST, \\ \frac{dLT}{dt} & = 0. \end{cases} \tag{4}$$

Thereafter, we also introduce a constant α_{LT} proliferation rate of long-lived T cells after each vaccination. Taking this into account, we obtain Model 5 where we assume equal expansion rates for ST after the two vaccinations, written as :

$$\begin{cases} \frac{dST}{dt} & = \alpha_{ST} I_{0\leq t\leq h_1} + \alpha_{ST} I_{2\leq t\leq h_2} - \mu_{ST} ST, \\ \frac{dLT}{dt} & = \alpha_{LT} I_{0\leq t\leq h_1} + \alpha_{LT} I_{2\leq t\leq h_2}. \end{cases} \tag{5}$$

We complete the T cell models with the Model 6, in which in each vaccination different ST activation rates are considered, given as:

$$\begin{cases} \frac{dST}{dt} & = \alpha_{1_{ST}} I_{0\leq t\leq h_1} + \alpha_{2_{ST}} I_{2\leq t\leq h_2} - \mu_{ST} ST, \\ \frac{dLT}{dt} & = \alpha_{LT} I_{0\leq t\leq h_1} + \alpha_{LT} I_{2\leq t\leq h_2}. \end{cases} \tag{6}$$

By incorporating this distinction and building it into our models, we can provide more accurate predictions and insights into how vaccines may elicit protective immunity. These insights are particularly relevant for the design of new vaccines and the assessment of long-term vaccine efficacy. The models presented here are thus not only mathematically robust but also deeply rooted in biological reality, making them a valuable tool for both theoretical and applied immunological research.

To put our modeling approach into perspective for a broader audience, we have developed models that simulate how T cells react and change over time in response to hepatitis B vaccination. These models help us understand the complex interactions within the immune system and predict how it responds to vaccines, crucial for designing effective immunotherapies and vaccination strategies.

2.4 Statistics

2.4.1 Nonlinear mixed models

Nonlinear mixed models are designed to capture the inter-individual variability in response to Hepatitis B vaccination, integrating both fixed effects to represent common trends and random effects to encapsulate individual deviations. Each individual parameter P_i can be described as $P_i = u_i P_{pop}$, where P_{pop} is a population parameter and u_i is log-normally distributed with $E(u_i) = 1$. To better reflect the underlying

biological processes and enhance model interpretability, we have meticulously justified the inclusion and definition of each parameter. Categorical variables, such as sex,are incorporated via dummy variables accompanied by an additional parameter β_j, which quantifies group-specific deviations from the reference category, enabling a nuanced exploration of the demographic influences on the parameter estimates. This allows for investigating which specific parameter of the structural model, such as expansion rate or decay rate, is responsible for observed differences between different groups.

The statistical methodology employed herein synergizes stochastic approximation of the standard expectation maximization algorithm (SAEM) with simulated annealing, combined with a Markov chain Monte Carlo (MCMC) approach that substitutes the simulation step of the SAEM algorithm. This robust fusion not only enhances the precision of parameter estimation but also fortifies the model against potential overfitting. The computation of the log-likelihood through importance sampling, assuming a fixed t-distribution with 5 degrees of freedom, provides a safeguard against data outliers, thereby bolstering the model's reliability. The extensive computational efforts undertaken using the facilities of the VSC (Vlaams Supercomputer Centrum) have facilitated a rigorous data analysis and modeling process, strengthening the confidence in our statistical outcomes. These statistical approaches extend beyond mere computational analysis, serving as vital tools for translating quantitative data into deeper biological understanding. This integration of statistical rigor and biological relevance elevates the impact of our findings, contributing significantly to the field of immunological research.

2.4.2 Inference and model selection

We have adopted a systematic and robust approach to model selection. nitially, a comprehensive suite of models, from Model 1 to Model 6, was created to analyze T-cell data. These models incorporated varying assumptions about parameter variability, explicitly accounting for whether individual variation was present, thus determining if random effects should be included for different parameters.In a first step, a list of models was composed, consisting of models 1 to 6 for T-cell data, together with assumptions on the parameters reflecting whether or not individual variation on these parameters is present, i.e. whether or not random effects were included for the different parameters. This selection was meticulously designed to reflect the intricate biological mechanisms governing T-cell responses. Parameters for these models were rigorously estimated using Monolix software ©Lixoft, a leading tool for such analyses.

Models with suboptimal SAEM convergence, generally indicative of undue complexity or poor data fit, were excluded from further analysis. The remaining models were then evaluated using Akaike's Information Criterion (AIC), with the model boasting the lowest AIC identified as the preliminary candidate. To solidify our model selection, a non-parametric bootstrap analysis with 1000 resamples was conducted on the leading model. This step underwent critical evaluation to ensure the resampling process accurately represented the variability within the data. By adopting a sequential approach that focused only on models with the most favorable AIC metrics enabled us to significantly reduce computational demands. This analysis revealed that a successful bootstrap required proper SAEM convergence in at least 70-80% of the samples. Consequently, we established that a minimum of 70% bootstrap sample convergence was necessary to consider the bootstrap analysis reliable. Models falling short of this benchmark were rigorously scrutinized and eliminated from the pool of potential candidates. For a detailed explanation of the underlying algorithms, the reader is referred to[14]. These algorithms were primarily executed using the default settings of the Monolix software. Finally, to ensure robust estimation of population parameters, we utilized a two-step SAEM-MCMC method, reinforcing the statistical integrity of our analysis.

In summary, our methodological advancements include the use of mixed-effects models for capturing individual variability, novel approaches in T-cell dynamics modeling, and a systematic model selection process that ensures both accuracy and simplicity.

3 Results

For the present study, all parameters were initially set as random and were later selected one by one to be fixed, driven by a robust combination of their statistical significance—as determined by the Akaike Information Criterion (AIC)—and their biological plausibility. This process was not only guided by statistical rigor but also by a clear relevance to the biological phenomena under study, as elaborated in the Mathematical Methods subsection 2.3. After a meticulous evaluation, each parameter was fixed, grounding our model in both theoretical and empirical validity. The selection of the fixed effects was anchored in a comprehensive analysis of their statistical robustness and theoretical underpinnings, as detailed in the Mathematical Methods subsection 2.3. Only those fixed effects that demonstrated unequivocal significance were incorporated into the tables 2 and 4, which were the product of a series of preliminary analyses involving various model iterations with different combinations of fixed and random parameters. This iterative and transparent process, as outlined in the Statistical Methods section 2.4, reinforces the robustness of our findings and directly addresses any concerns regarding the justification for parameter fixation. The meticulous and discerning selection process ensures that the fixed effects included in the final tables are not only meaningful but also enhance the overall scientific rigor of the study.

3.1 Conventional memory T-cells datasets (Tconv)

3.1.1 Model selection

The Tconv dataset was modeled using the model selection process described in section 2.4.2. Initially, we considered model 1 for Tconv, which assumes $\alpha_{1_T} = \alpha_{2_T} = \alpha_T$. Model 1a supposed that all parameters had random effects, resulting in an AIC value of 1727.23.

We then considered model 2, where $\alpha_{1_T} \neq \alpha_{2_T}$. Model 2a assumed that all parameters had random effects, resulting in a converged AIC value of 1705.11. When we introduced fixed effects for h_2, the model demonstrated a marginally lower AIC value of 1701.86 in model 2b.

Next, we assumed the distinction between short-lived and long-lived T cells (ST and LT), as justified in the subsection on Mathematical Methods 2.3. Model 3 assumed all parameters had random effects, while models 3b and 3c fixed u_{ST} and h_2, respectively. Only model 3a, with an AIC value of 1756.3, showed convergence.

Model 4 considered different expansion rates of T cells after each vaccination, reflecting the distinct immune response kinetics observed post-vaccination.. Model 4a considered random effects for all parameters, while models 4b and 4c fixed the expansion rates $\alpha_{1_{ST}}$ and $\alpha_{2_{ST}}$. Model 4d assumed the decay of T cells (μ_{ST}) occurred with a fixed population parameter. Models 4e and 4f fixed the period after each vaccination that T cells were activated for h_1 and h_2, respectively. SAEM convergence was only reached for model 4a and model 4c, with AIC values of 1651.33 and 1649.52, respectively.

Models 5 and 6 were obtained when LT activation with a constant proliferation rate was assumed, taking into account the established immunological knowledge. Model 5 assumed that the activation rates of ST were identical following each vaccination. This led to model 5a, with an AIC value of 1760.13, assuming all parameters were random. In model 5b, we assumed h_2 to be fixed population parameters, showing an AIC value of 1758.05. We did not achieve SAEM convergence in models with fixed population parameters u_{ST}, h_1, and α_{LT}.

The last model examined was model 6, in which different activation rates for ST were considered. We set all parameters as random parameters, leading to model 6a, with SAEM convergence reached and an AIC value of 1660.01. We set the decay rate of ST-cells (u_{ST}), proliferation rate of LT (a_{LT}), and activation periods (h_1 and h_2) as fixed parameters in models 6b, 6c, 6d, and 6e, respectively. We considered combinations of these fixed parameters but did not observe any improvement except for model 6e, with

SAEM convergence achieved and an AIC value of 1656.23.

Model 4c was initially chosen as the leading candidate model due to its lowest AIC value of 1649.52. However, it was later rejected as a result of a 1000-sample bootstrap that failed to demonstrate sufficient, this indicates that despite the low AIC value suggesting a good fit, the bootstrap results call into question the model's stability and predictive power, which is why Model 4c was ultimately not selected. Similarly, Models 6a and 6e also lacked proper bootstrap convergence. As a result, Model 4a

$$\begin{cases} \dfrac{dST}{dt} &= \alpha_{1_{ST}} I_{0\le t\le h_1} + \alpha_{2_{ST}} I_{2\le t\le h_2} - \mu_{ST} ST, \\ \dfrac{dLT}{dt} &= 0, \end{cases}$$

with an AIC value of 1651.33, was selected as a candidate model since it demonstrated bootstrap convergence with 95% of the bootstrap samples achieving SAEM convergence. A bootstrap convergence of 95% for Model 4a indicates that the model's predictions are stable across a wide range of resampled datasets, providing confidence in its reliability and predictive power. This high level of convergence suggests that the parameter estimates and model structure are robust, reinforcing our confidence in the biological and statistical interpretations discussed in the Statistics subsection 2.4. A thorough search was conducted in both the converging and non-converging bootstrap datasets for frequently deviant profiles, but none were identified. In summary, Model 4a indicates that the expansion rates of Tconv after the first and second vaccinations are distinct, and this observation may have implications for the long-term durability of vaccine-induced immunity. Moreover, the findings align with the theoretical insights into T-cell dynamics post-vaccination outlined in the Mathematical Methods section 2.3, suggesting the existence of two types of conventional memory T cells with one actively expanding and contracting after vaccination and the other remaining at a stable background equilibrium.

3.1.2 Covariate influence

The sequential approach to covariate analysis, starting with a fundamental model followed by incorporating covariates, was strategically chosen. This method ensures that the primary dynamics are well-understood before examining the nuanced influences of covariates, allowing for a clear distinction between primary effects and additional covariate impacts.

To understand the factors that could potentially influence the dynamics of conventional memory T-cells post-vaccination, we conducted an extensive investigation into a variety of covariates. These included biological indicators such as sex, age, and antibody titers; clinical factors like CMV, EBV, and HSV seropositivity; and demographic details such as the status of early or late converters. Our intent was to encompass a broad spectrum of variables that might exert influence over the immune response, to ensure a thorough examination of all plausible influences.

In this rigorous analysis, we tested each covariate for its impact on the parameters of our model. The covariates were chosen based on their potential biological and clinical importance, reflecting our aim to capture any significant contributors to the variability of the immune response following vaccination.

Our study included an unequal sex proportion (female 22: male 12), which could potentially affect the outcomes. However, in our analysis, sex was tested as a covariate and found to have no significant impact on the models, indicating that the immune response to the HBV vaccine in our study was not significantly influenced by the sex of the participants. We acknowledge the importance of sex-based differences and will aim for a more balanced sex ratio in future studies to further validate these findings.

On the selected model 4a, it is now possible to investigate the influence of some covariates. To decide which parameter-covariate relationship to test next, we used the Conditional Sampling usage for Stepwise

Tconv model	Fixed population parameter	Convergence-AIC	Candidate model	Bootstrap convergence
1a	–	1727.23	No	
2a	–	1705.11	No	
2b	h_2	1701.86	No	
3a	–	1756.3	No	
3b	μ_{ST}	No	No	
4a	–	1651.33	Selected	91%
4b	$\alpha_{1_{ST}}$	No	No	
4c	$\alpha_{2_{ST}}$	1649.52	Yes	No
4d	μ_{ST}	No	No	
4e	h_1	No	No	
4f	h_2	No	No	
5a	–	1760.13	No	
5b	h_2	1758.05	No	
6a	–	1660.01	Yes	73%
6e	h_1	1656.23	Yes	No

Table 2. ODE Model Formulations Considered for Memory Conventional T-Cell Data and Model Selection Procedure. The table details the fixed population parameter, convergence-AIC, candidate models, and bootstrap convergence for the six different Tconv models considered in the analysis. Model 4c and 6a were selected as the best models for the data, with 91% and 73% bootstrap convergence, respectively. The table provides important information about the model selection procedure for the Tconv models.

Approach based on Correlation testing (COSSAC) method that makes use of the data in the current model. The COSSAC method we employed is detailed in Ayral et al.[23], which provides a comprehensive guide to its application in model selection. By applying this method, the number of covariate models that are looked at is drastically reduced while the models that increase log-likelihood remain in the search. In particular, we investigated whether sex, age, antibody titres, TCR, early/late-converters, CMV, EBV and HSV seropositivity affect the model parameters.

The investigation revealed that adding the covariates of early/late-converters and HSV seropositivity, which effect on the parameter μ_{ST}, generated a more parsimonious model with a lower AIC of 1642.45, improving the AIC value of the original model selected by 8.68 points. The other covariates did not have a significant influence on model 4a. This significant improvement suggests a robust covariate effect, indicating that early/late-converters and HSV seropositivity may play an important role in the model. These results indicate that HSV1 carriership may be associated with lower expansion rates compared to non-carriers. Furthermore, early converters exhibit lower decay rates μ_{ST}, which could have implications for understanding the differential immune response dynamics among individuals. The estimated parameter values and corresponding 95% confidence intervals for the final model 4a are shown in Table 3, The p-values and confidence intervals provided alongside the parameter estimates in Table 3 offer a statistical basis for assessing the significance and reliability of the model parameters. This statistical evidence is crucial for the biological interpretation of the model, supporting the validity of the findings within the context of T-cell dynamics post-vaccination. Additionally, Figure 3 shows the comparison between the observations of T cells and the predictions from model 4a on linear scale and logarithmic scale. Figure

4 presents the Visual Predictive Check (VPC), demonstrating that the observed percentiles match the expected percentiles and remain within the prediction intervals.

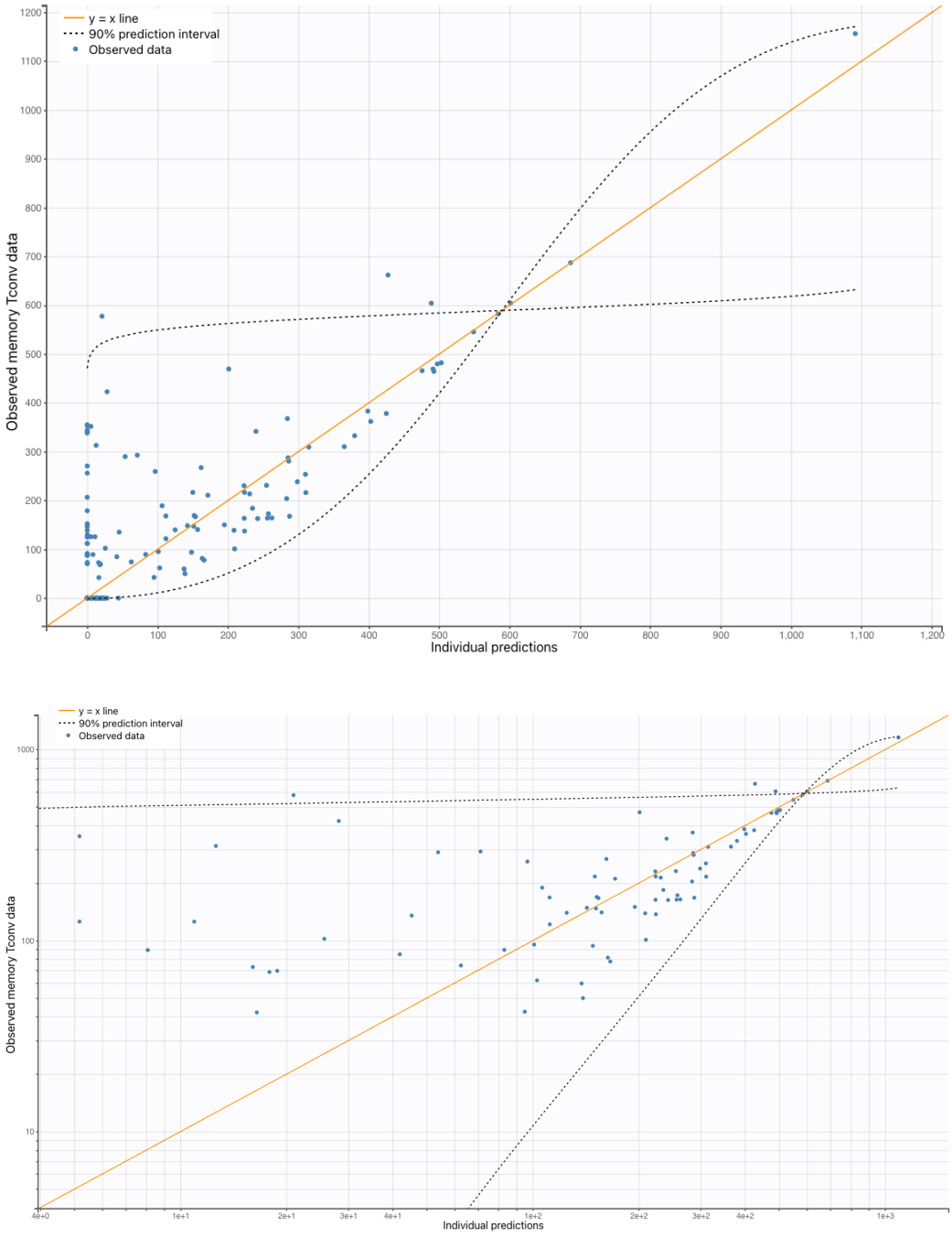

Figure 3. Comparison of observed memory conventional T-cell data (blue circles) with the predictions of model 4a (line).On top The dotted lines represent the 95% prediction interval on a linear scale. Down The dotted lines represent the 95% prediction interval on a logarithmic scale.

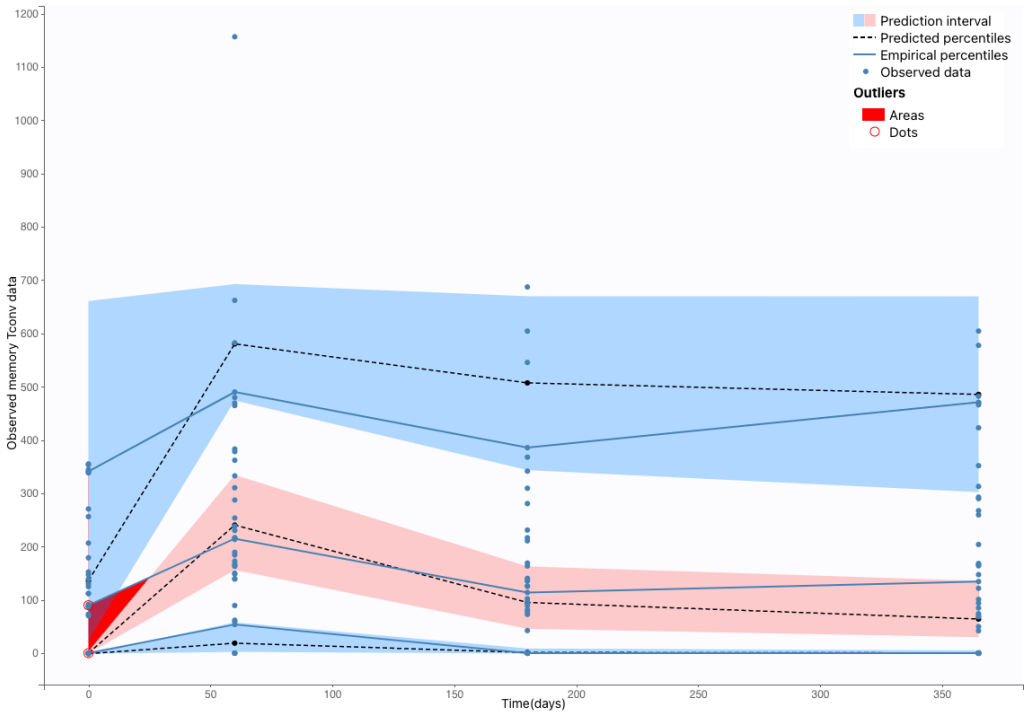

Figure 4. The Visual Predictive Check (VPC). We present a VPC to assess the performance of our model (Model 4a) in predicting Tconv data. The blue lines represent observed empirical percentiles summarizing the Tconv data from our study. The blue and pink shaded areas depict 95% prediction intervals generated by our model. Notably, the observed percentiles consistently fall within the 95% prediction intervals, indicating that our model provides a good fit to the observed data and is capable of capturing the variability present in the Tconv data.

Parameter	Estimate	95% CI	P-value
$T_{conv}(0)$	10976.43	(6.93 $e6$; 8.98 $e11$)	
$\alpha_{1_{ST}}$	10.65	(7.62; 31.689)	
$\alpha_{2_{ST}}$	3.13	(0.615 ; 7.053)	
$\beta_{\alpha_{2_{ST}}}(HSV1)$	-1.65	(-2.918; -0.292)	4.63e-16
u_{ST}	0.017	(0.006; 0.045)	
$\beta_{u_{ST}}(Late-converter)$	1.28	(0.18; 2.336)	3.04e-6
$\beta_{u_{ST}}(Non-converter)$	1.92	(0.719; 3.271)	4.08e-7

Table 3. Parameter estimates and corresponding 95% confidence intervals (CI) of final model 4a.

3.2 Regulatory memory T-cells datasets (Treg)

3.2.1 Model selection

Similarly as previously regarding the conventional memory T cells, we used model 1 to analyze the Treg dataset and observed the following distinctions: a scenario where all parameters have random effects led to model 1a, where an AIC value of 1592.31 was found. Setting α_T fixed in model 1b did not improve the model (AIC:1593.47). On the other hand, when we set fix μ_T, h_1 and h_2 we get a lower AIC value for

model 1c (AIC:1588.01), 1d (AIC:1590.1), 1e (AIC:1589.35), respectively.

Next, we considered model 2, which assumes a changed rate after the second vaccination due to a memory response. We obtained an AIC value of 1553.86 for model 2a, assuming all parameters had random effects. However, when we adapted the assumptions and considered fixed population parameters, the model did not improve in some cases and did not converge in others.

We further explored models that separated short-lived and long-lived T-cells. For model 3a, where all parameters were assumed to have random effects, we obtained an AIC value of 1599.76. However, no SAEM convergence was achieved for model 3b, where we fixed α_T. In models 3c, 3d, and 3e, we fixed mu_T, h_1, and h_2, respectively. Model 3c and 3e showed a lower AIC value, 1596.88 and 1596.75, respectively.

For model 4a, where all parameters were considered random, we obtained an AIC value of 1559.85. When we set α_{1_T}, α_{2_T}, and μ_{ST} as fixed parameters in models 4b, 4c, and 4d, respectively, we did not achieve SAEM convergence. No significant result was obtained when setting other parameters fixed.

We also considered models 5 and 6, which include a proliferation rate for LT. For model 5, many assumptions were made about the parameters, but we did not obtain convergence. Finally, we examined model 6. When testing different assumptions about the parameters, only model 6a and model 6f showed convergence. In model 6a, all parameters had random effects, leading to an AIC value of 1567.3. In model 6f, h_2 was set as a fixed parameter, giving an AIC value of 1564.35.

The model 2a had the lowest AIC value of 1545.8 among all the above-mentioned models

$$\frac{dT}{dt} = \alpha_{1_T} I_{0\leq t\leq h_1} + \alpha_{2_T} I_{2\leq t\leq h_2} - \mu_T T,$$

and was selected as the first candidate model. The candidate model showed bootstrap convergence; 93% of the bootstrap samples achieved SAEM convergence, this high percentage of convergence in bootstrap samples reinforces the validity of Model 2a, suggesting that it is a stable and reliable representation of the underlying biological processes. As before, we examined often divergent profiles in the converging and non-converging bootstrap datasets, but no such profile was detected. This suggests that the model is robust and that the results are reliable. Overall, these results indicate that model 2a is a strong candidate for explaining the underlying data and that it can be used to make predictions or draw conclusions about the phenomenon being studied. We note that model 2a is similar to model 4a with the difference of no co-existence of a stable background population.

3.2.2 Covariate influence

Similar to our approach with conventional memory T-cells, we evaluated a comprehensive set of covariates for regulatory memory T-cells. This encompassed demographic, clinical, and biological factors that could modulate the immune system's behavior in response to vaccination, such as age, sex, and seropositivity to various viruses like CMV, EBV, and HSV. The selection of these covariates was informed by their hypothesized relevance to the dynamics of T-cell populations post-vaccination.

Upon examining the influence of each covariate within our model framework, we identified specific factors that significantly altered the model parameters, thus providing insights into the differential immune responses observed among individuals.

Our sample included more females (22) than males (12), which raised concerns about potential sex-related biases in the outcomes. However, after including sex as a covariate in the analysis, we found that sex did not significantly affect the models.

We applied the COSSAC approach, a method that strategically narrows down covariate models to those that most significantly improve the log-likelihood, as detailed in Ayral et al[23]. The model that

Treg model	Fixed population parameter	Convergence-AIC	Candidate model	Bootstrap convergence
1a	–	1592,31	No	
1b	α_T	1593.47	No	
1c	h_2	1588.01	No	
2a	–	1545.80	Selected	93%
2b	α_{1_T}	1548.28	Yes	82%
2c	α_{2_T}	1553.11	No	
2d	μ_T	1551.67	Yes	72%
2e	h_1	1572.98	No	
3a	–	1599.76	No	
3b	α_{ST}	No	No	
3c	μ_T	1596.88	No	
3e	h_2	1596.75	No	
4a	–	1559.85	Yes	No
4b	α_{1_T}	No	No	
4e	h_1	1571.15	No	
6a	–	1567.30	No	
6b	$\alpha_{2_{ST}}$	No	No	
6e	h_1	1565.35	No	

Table 4. ODE Model formulations considered for memory conventional T-cell data and model selection procedure. Model 5 has been omitted from the table because non-convergence was obtained for random or fixed parameters.

examined early/late converters, adding the effect on the parameter μ_{ST}, and EBV seropositivity, adding the effect on the initial value of α_{2T}, was discovered to have the lowest AIC of 1536.89, decreasing the AIC value to the original model chosen by approximately 9 points. The estimated parameters and their 95% confidence intervals for the final Model 2a, which includes the effect of early/late converters and EBV seropositivity on the initial values of μ_{ST} and α_{2T}, respectively, are shown in Table 5, the inclusion of p-values and confidence intervals for the parameter estimates in Table 5 is not just for statistical rigor but also for biological relevance, allowing us to draw more confident conclusions about the role of these parameters in the regulatory T-cell dynamics post-vaccination. Figure 5 shows the comparison between the observations of T cells and the predictions from model 2a on both linear and logarithmic scale. Figure 6 presents the visual predictive check (VPC) comparing the model-based simulations with observed data. The VPC plot shows that the observed percentiles are close to the predicted percentiles and remain within the corresponding 95% prediction intervals, indicating that the model can accurately predict the immune response.

The results suggests that individuals who have been previously infected with EBV may have a different immune response to vaccination compared to those who have not been infected. Specifically, our study found that EBV seropositivity was associated with an increase in Treg cell expansion rates following vaccination, potentially enabling the virus to establish a stable infection by persisting within an individual.

Furthermore, the results also suggest that the dynamics of Treg cells may be influenced by the timing of their conversion. Specifically, individuals who convert to a positive response to the vaccine earlier have lower decay rates of Treg cells compared to late converters. We note that this finding is similar to what we

found for Tconv.

Parameter	Estimate	95% CI	P-value
$T_{reg}(0)$	13.13	(0.812;27.418)	
α_{1_T}	7062.06	(612.503;296344.9)	
α_{2_T}	4.3	(0.769;11.013)	
$\beta_{\alpha_{2_{ST}}}(EBV)$	-1.4	(-3.801;-0.163)	<2.2e-16
u_{ST}	0.038	(0.009, 0.083)	
$\beta_{u_{ST}}(Late-converter)$	1.76	(1.105, 2.985)	1.87e-14

Table 5. Parameter estimates and corresponding 95% confidence intervals (CI) of final model 2a.

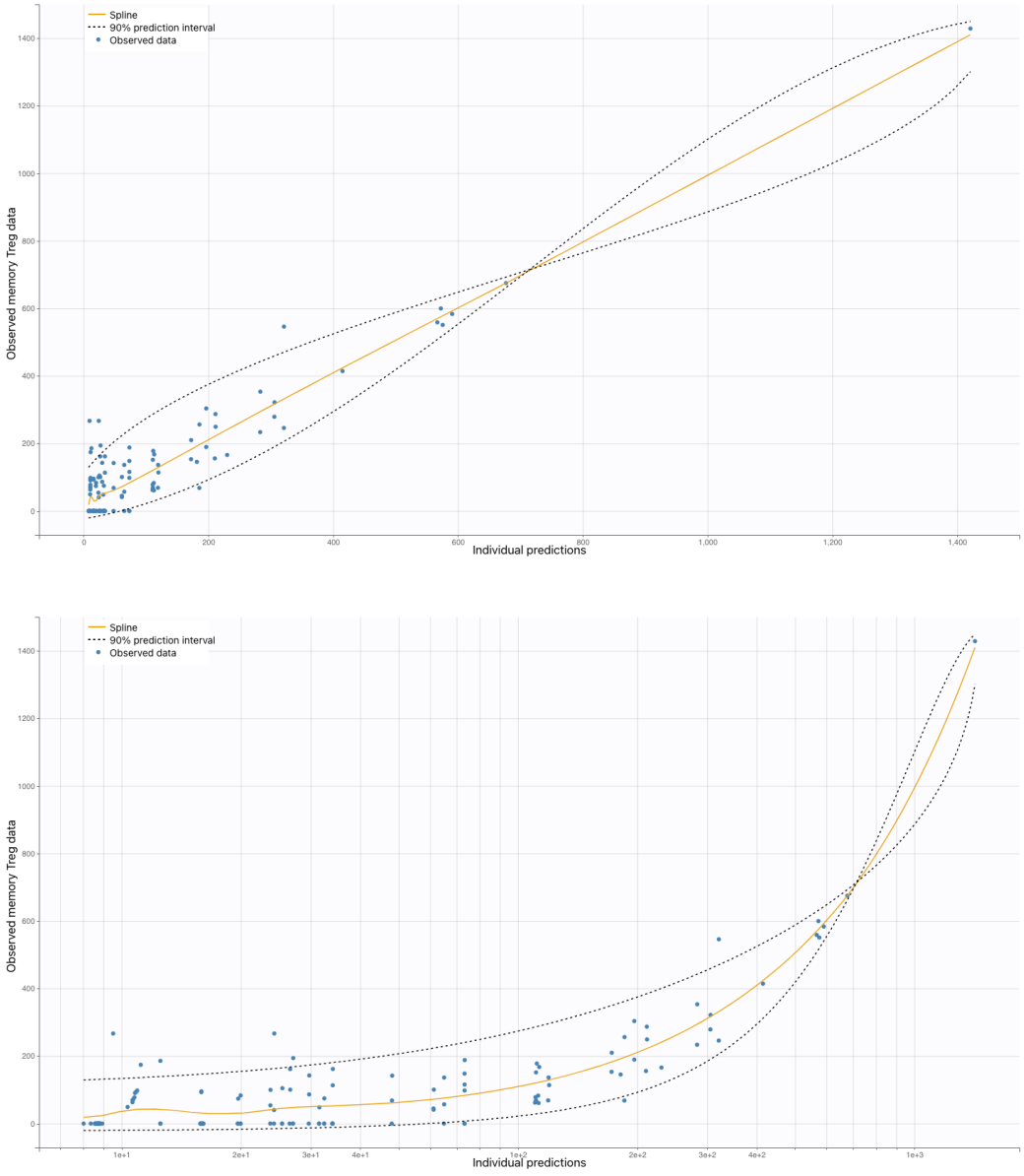

Figure 5. Comparison of observed memory regulatory T-cell data (blue circles) with the predictions of model 2a (line). On top The dotted lines represent the 95% prediction interval on a linear scale. Down The dotted lines represent the 95% prediction interval on a logarithmic scale.

4 Discussion and conclusion

Understanding the establishment of effective immunological memory is a complex task. In this study, we employed mixed-effects modeling to analyze data from a previously published vaccination trial featuring de novo Hepatitis B surface antigen-specific CD4 T cells[9]. This approach enabled us to identify individual variations in immune responses and discern the diverse dynamics observed in Tconv and Treg cells post-vaccination. By applying ordinary differential equations, we unveiled two pivotal models that significantly contribute to our understanding of T cell memory formation in response to the hepatitis B vaccine.

(i) Regarding conventional T cells, our best model (referred to as model refM4) demonstrated that the

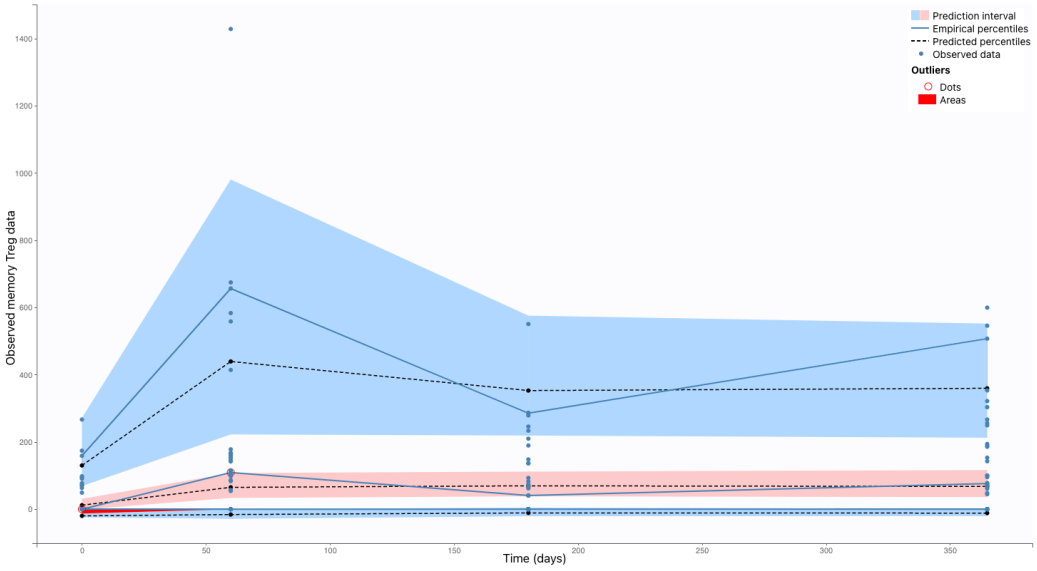

Figure 6. The Visual Predictive Check (VPC) comparing the results of the model-based simulations with observed data. We present a VPC to assess the performance of our model (Model 2a) in predicting Treg data. The blue lines represent observed empirical percentiles summarizing the Treg data from our study. The blue and pink shaded areas depict 95% prediction intervals generated by our model. Notably, the observed percentiles consistently fall within the 95% prediction intervals, indicating that our model provides a good fit to the observed data and is capable of capturing the variability present in the Treg data.

dynamics of Tconv consist of two types of memory T-cells with actively expanding and contracting and the other remaining unchanged at a stable level. Moreover the dynamic Tconv type was influenced by the Early/Late converter status and HSV-1 seropositivity. It was observed that early converter vaccinees had lower decay rates for short lived Tconv cells, compared to late converter vaccinees and non-converters . This is supported by the finding in the Elias et al[9] study, indicating that early-converters have a higher relative frequency of vaccine-specific TCRβ sequences present in their conventional memory CD4 T cell repertoire at day 60 compared to vaccinees from the two other groups in the cohort. Our modeling results thus allow us to add knowledge on why these higher T-cell frequencies could have been established on day 60. In contrast to a potentially more rapid T-cell expansion in early converters, our modeling actually indicated that the higher frequency in early converters could be a consequence of a lower T cell decay rate in early converters compared to the two other converter groups .

Furthermore, the expansion rate after the second vaccination of the short lived Tconv cells was influenced by HSV-1 seropositivity, where the vaccinees without HSV-1 have a significantly higher expansion rate) compared to vaccinee who have HSV-1). Although other human herpesviruses have been noted to affect T cell responses upon vaccination (like CMV[24]), HSV-1 has not yet been reported by previous research. This could be suggesting that HSV-1 has the potential to modulate T-cell viability. Interestingly, HSV-infected cells have been reported to resist T-cell-induced apoptosis[25], which may be a mechanism behind the observed effect.

(ii) Regarding regulatory T cells, our best model (referred to as model 2) indicated no existence of a stable unchanged second Treg type next to the expanding and contracting Treg type. Our modeling

indicated that the Treg expansion rate after the second vaccination for individuals with positive EBV seropositivity was higher than for those without it, thereby suggesting that EBV might induce Treg activity. Tregs are a type of immune cell that play a role in regulating the immune response and preventing autoimmune reactions. However, if their activity is too high, they may suppress the immune response to viral infections. This, in turn, could contribute to a higher level of virus in the body over time and facilitate the establishment and maintenance of viral persistence for EBV This hypothesis is based on observed data trends but requires further research for confirmation. Our findings align with previous studies[26–28] and stimulate further investigation into the virus-host immune interactions. Additionally, our analysis showed that the time it took for individuals to convert to a positive response to the vaccine (i.e., early converters vs. late converters) was associated with differences in Treg cell decay rates. Specifically, individuals who convert to a positive response to the vaccine earlier have lower decay rates of Treg cells compared to late converters. Hypothetically, like in Tconv, better TCR-epitope recognition could have rendered a lower Treg decay rate, but this hypothesis would only be valid if the TCR-epitope recognition for Tconv would be correlated with Treg cellular regulation, which still remains to be proven. However, We found a slightly significant effect of TCR on the decay rate of Treg cells in our analysis, but due to lack of data for some individuals and instability in the bootstrap, we were unable to include it in our final model. It is possible that differences in TCR could still influence Treg cell activity in a subtle or complex manner, and further research is required to better understand its role in Treg cell dynamics.

After exploring the complexities of Tconv and Treg cell dynamics and their implications for immunological memory and vaccine efficacy, our findings underscore the need for broader investigation. These insights not only improve our understanding of Tconv and Treg cell dynamics following vaccination but also pave the way for more comprehensive studies of immune memory interpretation. The distinct roles of other immune cell populations beyond Tconv and Treg cells require further investigation to fully unravel the complexity of vaccine-induced immunity. This knowledge is pivotal for designing vaccines that ensure robust and lasting immunity.

Addressing the limitations of our study is essential for future research. The data used in this study were collected by Elias et al.[9], who utilized markers such as CD154 (CD40L) and CD137 (4-1BB) to identify activated T cells, including Tregs. Our focus on Tconv and Treg cells and the simplifications inherent in our modeling approach suggest that a broader examination of immune cell types and the use of comprehensive datasets are crucial steps towards a more detailed understanding of vaccine responses.Therefore, our findings should be viewed as a foundation for further research, which is needed to validate and extend our models.

In summary, our mixed effects modeling approach, based on ordinary differential equations, identified key factors influencing effective immunological memory in Tconv and Treg. Our study provides novel quantitative evaluation of T-cell dynamics temporal scales, offering insights into crucial biological processes unattainable with traditional statistics. We seamlessly integrated phenomenological elements with mechanistic models to elucidate the kinetics and drivers of T cell memory formation.

Our investigation reveals groundbreaking insights into the modulation of Tconv and Treg cell dynamics by external factors such as HSV-1 seropositivity and EBV. This advance in our understanding of vaccine-induced immunological memory underscores the potential for designing personalized vaccine strategies

Furthermore, our findings enhance understanding of the long-term dynamics of vaccine-induced immunity. Identifying key factors that influence sustained immune protection enables predictions of immune response development over time. This knowledge is invaluable for clinical trial researchers, aiding in the creation of more effective vaccination strategies and identifying individuals who may benefit

from additional interventions.

In conclusion, while our study has shed light on the unique responses of Tconv and Treg cells to vaccination, it also highlights the necessity for a broader perspective on immune cell dynamics in response to vaccines. Moving forward, it is imperative to expand our models to incorporate a wider range of data and immune cell types, thereby refining our strategies for immunological intervention.

Acknowledgements

We would like to express our gratitude to Geert Mortier and Viggo Van Tendeloo for their valuable contributions and assistance in this research.

Funding

BO acknowledges funding received from the European Research Council (ERC) under the European Union's Horizon 2020 research and innovation programme (grant agreement 851752-CELLULO-EPI) and Research Foundation Flanders (FWO) (grant agreement 1861219N). PB and PVD received UAntwerp funding (Methusalem and concerted research action).

References

1. Pulendran, B. & Li, S. Systems vaccinology. *Immunity* **33**, 516–529 (2010).

2. Murphy, K., Weaver, C. & Mowat, A. *Immunobiology: the immune system in health and disease* (Garland Science, 2017), 9th edn.

3. Sallusto, F., Geginat, J. & Lanzavecchia, A. Memory t cells. *Annu. review immunology* **22**, 745–763 (2010).

4. Thornton, A. M. & Shevach, E. M. Regulation of t cell-mediated immune responses by T cells. *Front. bioscience* **2**, E376–E389 (2010).

5. Surh, C. D. & Sprent, J. Regulation of T cell memory by cytokines. *Nat. reviews immunology* **8**, 247–258 (2008).

6. Harty, J. T. & Badovinac, V. P. Cellular and molecular basis of memory T-cell mediated immunity. *Adv. experimental medicine biology* **452**, 123–135 (2000).

7. Plotkin, S. A. Vaccines: correlates of vaccine-induced immunity. *Clin. infectious diseases* **67**, 205–209 (2018).

8. Zuckerman, J. N. *et al.* Immunogenicity, safety, and tolerability of a recombinant hepatitis B vaccine manufactured in mammalian cells. *Hum. vaccines* **1**, 232–238 (2004).

9. Elias, G. *et al.* Preexisting memory CD4 t cells in naïve individuals confer robust immunity upon hepatitis b vaccination. *eLife* **11**, 10.7554/elife.68388 (2022).

10. Hepatitis b vaccines: WHO position paper—recommendations. *Vaccine* **28**, 589–590, 10.1016/j.vaccine.2009.10.110 (2010).

11. Wenzel, J. J. & Jilg, W. Loss of antibodies, but not of protection. *The Lancet Infect. Dis.* **10**, 738–739, 10.1016/s1473-3099(10)70217-6 (2010).

12. Carrat, F. *et al.* Time lines of infection and disease in human influenza: A review of volunteer challenge studies. *Am. J. Epidemiol.* **167**, 775–785, 10.1093/aje/kwm375 (2008).

13. Perelson, A. S., Neumann, A. U., Markowitz, M., Leonard, J. M. & Ho, D. D. Hiv-1 dynamics in vivo: Virion clearance rate, infected cell life-span, and viral generation time. *Science* **271**, 1582–1586, 10.1126/science.271.5255.1582 (1996). https://www.science.org/doi/pdf/10.1126/science.271.5255.1582.

14. Lavielle, M. & Mentré, F. Estimation of population pharmacokinetic parameters of saquinavir in HIV patients with the MONOLIX software. *J. Pharmacokinet. Pharmacodyn.* **34**, 229–249, 10.1007/s10928-006-9043-z (2007).

15. Wakefield, J. & Racine-Poon, A. An application of bayesian population pharmacokinetic/pharmacodynamic models to dose recommendation. *Stat. Medicine* **14**, 971–986, https://doi.org/10.1002/sim.4780140917 (1995).

16. Andraud, M. *et al.* Living on three time scales: The dynamics of plasma cell and antibody populations illustrated for hepatitis a virus. *PLoS Comput. Biol.* **8**, e1002418, 10.1371/journal.pcbi.1002418 (2012).

17. Pasin, C. *et al.* Dynamics of the humoral immune response to a prime-boost ebola vaccine: Quantification and sources of variation. *J. Virol.* **93**, 10.1128/jvi.00579-19 (2019).

18. Le, D., Miller, J. D. & Ganusov, V. V. Mathematical modeling provides kinetic details of the human immune response to vaccination. *Front. Cell. Infect. Microbiol.* **4** (2015).

19. Keersmaekers, N., Ogunjimi, B., Damme, P. V., Beutels, P. & Hens, N. An ODE-based mixed modelling approach for b- and t-cell dynamics induced by varicella-zoster virus vaccines in adults shows higher t-cell proliferation with shingrix than with varilrix. *Vaccine* **37**, 2537–2553, 10.1016/j.vaccine.2019.03.075 (2019).

20. Besbassi, H. *et al.* Nonlinear mixed models for varicella-zoster virus specific antibody dynamics following clinical herpes zoster. *Front. Immunol.* **14**, 10.3389/fimmu.2023.1104605 (2023).

21. Garcia-Fogeda, I. *et al.* Within-host modeling to measure dynamics of antibody responses after natural infection or vaccination: A systematic review. *Vaccine* **41**, 3701–3709, 10.1016/j.vaccine.2023.04.030 (2023). Epub 2023 May 16.

22. Schoenbrunn, A. *et al.* A converse 4-1bb and cd40 ligand expression pattern delineates activated regulatory t cells (treg) and conventional t cells enabling direct isolation of alloantigen-reactive natural foxp3+ treg. *J. Immunol.* **189**, 5985–5994, 10.4049/jimmunol.1201090 (2012).

23. Ayral, G., Si Abdallah, J.-F., Magnard, C. & Chauvin, J. A novel method based on unbiased correlations tests for covariate selection in nonlinear mixed effects models: The cossac approach. *CPT: Pharmacometrics & Syst. Pharmacol.* **10**, 318–329, https://doi.org/10.1002/psp4.12612 (2021). https://ascpt.onlinelibrary.wiley.com/doi/pdf/10.1002/psp4.12612.

24. Furman, D. *et al.* Cytomegalovirus infection enhances the immune response to influenza. *Sci. translational medicine* **7**, 281ra43–281ra43 (2015).

25. Jerome, K. R. *et al.* HSV and glycoprotein j inhibit caspase activation and apoptosis induced by granzyme b or fas. *The J. Immunol.* **167**, 3928–3935, 10.4049/jimmunol.167.7.3928 (2001).

26. Wingate, P., McAulay, K., Anthony, I. & Crawford, D. Regulatory t cell activity in primary and persistent epstein-barr virus infection. *J. Med. Virol.* **81**, 870–877, 10.1002/jmv.21445 (2009).

27. Li, J., Qian, C.-N. & Zeng, Y.-X. Regulatory t cells and EBV associated malignancies. *Int. Immunopharmacol.* **9**, 590–592, 10.1016/j.intimp.2009.01.015 (2009).

605 **28.** Rosenblum, M. D., Way, S. S. & Abbas, A. K. Regulatory t cell memory. *Nat. Rev. Immunol.* **16**,
606 90–101, 10.1038/nri.2015.1 (2015).